Nanocrystalline Aluminum Nitride and Aluminum/Gallium Nitride Nanocomposites via Transamination of $[M(NMe_2)_3]_2$, M = Al, Al/Ga (1/1)

Jerzy F. Janik† and Richard L. Wells*

Department of Chemistry, Paul M. Gross Chemical Laboratory, Duke University, Durham, North Carolina 27708-0346

Jeffery L. Coffer and John V. St. John

Department of Chemistry, Texas Christian University, Ft. Worth, Texas 76129

William T. Pennington and George L. Schimek

Department of Chemistry, Clemson University, Clemson, South Carolina 29634

Received December 17, 1997. Revised Manuscript Received March 30, 1998

Reactions of $[Al(NMe_2)_3]_2$ with NH_3, mimicking the case of the related Ga-derivative, provided an Al−amide−imide precursor that was pyrolyzed to pure nanocrystalline AlN. Based on that chemistry, a mixed Al/Ga precursor system was designed to lead to the bimetallic nitride composites. A prototype study included equilibration in hexane or toluene of the dimers $[M(NMe_2)_3]_2$, M = Al, Ga, which resulted in the formation of the homoleptic four-membered-ring compound $(Me_2N)_2Al(\mu\text{-}NMe_2)_2Ga(NMe_2)_2$. Crystalline $[M(NMe_2)_3]_2$, M = Al/Ga (1/1), obtained from this equilibration was structurally characterized. Transamination/deamination reactions carried out with liquid NH_3 in the preequilibrated bimetallic system $[Al(NMe_2)_3]_2/[Ga(NMe_2)_3]_2$, Al/Ga = 1/1, resulted in the mixed M−amide−imide precursors that were converted at 700−1100 °C to aluminum/gallium nitride nanocomposite materials. The nature of these bulk nanocomposites has been elucidated by XRD, TEM/EDS, IR, and PL techniques.

Introduction

Some group 13 nitrides such as BN and AlN are promising ceramic materials,[1] and others are advantageous semiconductors[2] with a direct band gap from 1.4 eV (InN) to 3.4 eV (GaN) or to 6.2 eV (AlN). However, new technological applications require materials with tunable electronic/crystalline properties and improved ceramic features. For example, the first demand is encountered in advanced blue LEDs and blue laser designs which employ nitride's solid solution films with appropriate crystalline properties.[2] On the ceramic application side, nitride solid solutions and composite materials are expected to possess unique and often improved properties over pure components.[1b,3] In this regard, it is generally recognized that classical bulk syntheses of these materials have intrinsic limitations to achieve many of the challenging goals, and the problems' solutions are sought in precursor design and thermoprocessing.

We recently demonstrated that transamination/deamination reactions at ambient conditions between $[Ga(NMe_2)_3]_2$ and NH_3 afforded the gallium imide $[Ga(NH)_{3/2}]_n$, which was pyrolyzed to high-purity nanocrystalline GaN.[4] Related chemistry has also been reported for making thin films of such main-group nitrides as GaN,[5a] AlN,[5b] Si_3N_4,[5c] and Sn_3N_4.[5d] In all of these systems, it is convenient to think that the primary transamination product, the transient and unstable metal (M) amide, $M(NH_2)_x$, undergoes a stepwise elimination−condensation process, deamination, as

* Correspondence to this author.

† On leave from the University of Mining and Metallurgy, Krakow, Poland.

(1) For example, see the following (and references therein): (a) Paine, R. T. *J. Inorg. Organomet. Polym.* **1992**, *2*, 183. (b) Sauls, F. C.; Interrante, L. V. *Coord. Chem. Rev.* **1993**, *128*, 193. (c) Sheppard, L. M. *Am. Ceram. Soc. Bull.* **1990**, *69*, 1801. (d) Baker, R. T.; Bolt, J. D.; Reddy, G. S.; Roe, D. C.; Staley, R. H.; Tebbe, F. N.; Vega, A. J. *Mater. Res. Soc. Symp. Proc.* **1988**, *121*, 471.

(2) For example, see the following reviews: (a) Nakamura, S. *Mater. Sci. Eng.* **1997**, *B43*, 258. (b) Morkoç, H. *Mater. Sci. Eng.* **1997**, *B43*, 137. (c) Akasaki, I.; Amano, H. *J. Cryst. Growth* **1997**, *175/176*, 29.

(3) (a) Paine, R. T.; Janik, J. F.; Fan, M. *Polyhedron*, **1994**, *13*, 1225 and references therein. (b) Kwon, D.; Schmidt, W. R.; Interrante, L. V.; Marchetti, P.; Maciel, G. In *Inorganic and Organometallic Oligomers and Polymers;* Harrod, J. F., and Laine, R. M., Eds; Kluwer Academic Press: Hingham, MA, 1991; p 191. (c) Mazdiyasni, K. S.; Ruh, R.; Hermes, E. E. *Am. Ceram. Soc. Bull.* **1985**, *64*, 1149. (d) Twait, D. J.; Lackey, W. J.; Smith, A. W.; Lee, W. Y.; Hanigofsky, J. A. *J. Am. Ceram. Soc.* **1990**, *73*, 1510.

(4) (a) Janik, J. F.; Wells, R. L. *Chem. Mater.* **1996**, *8*, 2708. (b) Wells, R. L.; Janik, J. F.; Gladfelter, W. L.; Coffer, J. L.; Johnson, M. A.; Steffey, B. D. *Mater. Res. Soc. Symp. Proc.* **1997**, *468*, 39. (c) Coffer, J. L.; Johnson, M. A.; Zhang, L.; Wells, R. L.; Janik, J. F. *Chem. Mater.* **1997**, *9*, 2671. (d) Wells, R. L.; Gladfelter, W. L. *J. Cluster Sci.* **1997**, *8*, 217.

(5) (a) Hoffman, D. M. *Polyhedron* **1994**, *8*, 1169. (b) Gordon, R. G.; Hoffman, D. M.; Riaz, U. *Mater. Res. Soc. Symp. Proc.* **1991**, *204*, 95. (c) Gordon, R. G.; Hoffman, D. M.; Riaz, U. *Chem. Mater.* **1990**, *2*, 480. (d) Riaz, U.; Gordon, R. G.; Hoffman, D. M. *Chem. Mater.* **1992**, *4*, 68.

S0897-4756(97)00806-5 CCC: $15.00
Published on Web 05/16/1998

illustrated for group 13 in eq 1:

$$\underset{\text{amide}}{M(NH_2)_3} \xrightarrow[-NH_3]{\Delta} \underset{\text{amide-imide}}{M(NH_2)(NH)} \xrightarrow[-1/2\ NH_3]{\Delta} \underset{\text{imide}}{M(NH)_{3/2}} \xrightarrow[-1/2\ NH_3]{\Delta} \underset{\text{nitride}}{MN} \quad (1)$$

Whereas at ambient conditions for M = Ga the elimination approaches the polymeric imide stage, there is evidence that for M = Al[6a,b] or Sn[6c] a room-temperature-stable form could be close to the polymeric amide−imide, $[M(NH_2)(NH)]_n$. In practice, as the cross-linking of the M−N network progresses into the condensed solid phase, the deamination may encounter severe kinetic barriers to reach any of the distinct stages. This may result in precursors with entrapped residual NR_2 groups. Appropriate pyrolysis conditions, such as a NH_3 atmosphere, could then be used to minimize residual carbon in the nitride material.

The chemistry outlined above provokes an interesting idea of a bimetallic (or higher) group 13−amide−imide precursor from a solution mixed molecular system $[M(NR_2)_3]_2/[M'(NR_2)_3]_2$. In a favorable case of efficiently coupled M−N(R$_2$)−M′ linkages, transamination with NH_3, and the resultant transient NH_2 functionalities, could lead via deamination to homogeneously dispersed and cross-linked M−N(H)−M′ bonds. The molecular level of homogeneity of such a mixed precursor coupled with abundant NH_2/NH M-bonded groups would present an outstanding opportunity for conversion to molecularly mixed nitrides. In this regard, hexagonal forms of AlN and GaN are known to form solid solutions for a full range of compositions, at least in AlGaN thin films from vapor deposition and molecular beam epitaxy techniques.[2,7] On the other hand, GaN and InN appear to form a more complex binary system with a miscibility gap.[8]

Herein, we first describe a successful preparation at ambient conditions of the solid Al−amide−imide from the transamination/deamination in the $[Al(NMe_2)_3]_2/NH_3$ system. This advantageous precursor was converted to high-purity, bulk nanocrystalline AlN. Further, we discuss equilibration in hydrocarbon and aromatic solvents of the bimetallic system $[Al(NMe_2)_3]_2/[Ga(NMe_2)_3]_2$ that results in the formation of the novel equilibrated four-membered-ring compound $(Me_2N)_2Al(\mu\text{-}NMe_2)_2Ga(NMe_2)_2$, which has been characterized by NMR spectroscopy. Transamination/deamination reactions with NH_3 were performed in the mixed system $[Al(NMe_2)_3]_2/[Ga(NMe_2)_3]_2$ to yield homogeneous Al/Ga−amide−imide precursors that were pyrolyzed to bulk aluminum/gallium nitride nanocomposites.

Experimental Section

General Techniques. All experiments were performed using standard vacuum/Schlenk techniques. Solvents were distilled from sodium benzophenone ketyl or Na/K alloy prior to use. $[Ga(NMe_2)_3]_2$[9a] and $[Al(NMe_2)_3]_2$[9b] were prepared by literature methods. Anhydrous NH_3 over Na was transferred to a reaction vessel at −196 or −78 °C; for pyrolysis experiments, NH_3 slowly evaporated into the pyrolysis tube that contained a precursor in a quartz boat and left the system through a bubbler. ^1H and $^{13}C\{^1H\}$ NMR spectra were recorded on a Varian Unity 400 at 25 °C from toluene-d_8, benzene-d_6, or hexane-d_{14} (with internal benzene-d_6) solutions and referenced vs $SiMe_4$ by generally accepted methods; ^1H VT NMR data were obtained from 25 to 90 °C using a toluene-d_8 solution. Mass spectra were collected on a JEOL JMS-SX 102A spectrometer, EI mode, at 20 eV. IR spectra of solids were acquired using KBr pellets on a BOMEM Michelson MB-100 FT-IR spectrometer. TGA/DTA data were acquired under a UHP nitrogen flow at a heating rate of 5 °C/min on a TA Instruments SDT 2960 simultaneous TGA/DTA apparatus. Elemental analyses were provided by E+R Microanalytical Laboratory, Corona, NY. Melting points (uncorrected) were determined with a Thomas-Hoover Uni-melt apparatus for samples flame-sealed in glass capillaries. Single-crystal X-ray diffraction study for $[M(NMe_2)_3]_2$, M = Al/Ga (1/1), was performed at Clemson University, Clemson, SC, on a Nicolet R3m/V diffractometer using graphite-monochromated Mo Kα radiation (λ = 0.71073 Å).[10] All calculations were carried out using the SHELXTL suite of programs;[11] the structure was solved by direct methods. XRD data were collected using mineral oil coated samples on a Phillips XRD 3000 diffractometer utilizing Cu Kα radiation; the average particle size, D, was calculated using the Scherrer equation[12] applied to low angle diffraction peaks. HRTEM microscopy (Topcon EM002B with a 200-kV accelerating voltage) and energy-dispersive spectroscopy, EDS (Topcon EM002B and Noran modem with an ultrathin window), were performed at the Analytical Instrumental Facility of North Carolina State University, Raleigh. Room-temperature photoluminescence (PL) data were recorded using a SPEX Flurolog-2 instrument equipped with a double-emission monochromator and an R928 photomultiplier tube. Excitation was provided by a 450-W Xe lamp whose output was focused into a 0.22-m monochromator to provide an excitation wavelength of 325 nm.

Preparation of the Al−Amide−Imide Precursor. A sample of powdered $[Al(NMe_2)_3]_2$, 1.59 g (5.0 mmol), was placed in a 100-mL flask, and 30 mL of liquid NH_3 was condensed onto it at −78 °C. The slurry was stirred at this temperature for 2 h and then refluxed in liquid NH_3 for 6 h. This was followed by a 2-h NH_3 boil-off yielding a white powdery solid, polymeric Al−amide−imide. The precursor was evacuated overnight. IR (cm^{-1}), broad bands: 680 (s), 802 (sh), 900 (s), 1018 (sh), 1262 (w), 1510 (w, sh), 1545 (m), 2775 (vw), 2857

(6) (a) Wiberg, E.; May, A. *Z. Naturforsch.* **1955**, *10b*, 229. (b) Maya, L. *Adv. Ceram. Mater.* **1986**, *1*, 150. (c) Maya, L. *Inorg. Chem.* **1992**, *31*, 1958.

(7) (a) Hagen, J.; Metcalfe, R. D.; Wickenden, D.; Clark, W. *J. Phys. C: Solid State Phys.* **1978**, *11*, L143. (b) Baranov, B.; Däveritz, L.; Gutan, V. B.; Jungk, G.; Neumann, H.; Raidt, H. *Phys. Stat. Solidi A* **1978**, *49*, 629. (c) Angerer, H.; Ambacher, O.; Stutzmann, M.; Metzger, T.; Höpler, R.; Born, E.; Bergmaier, A.; Dollinger, G. *Mater. Res. Soc. Symp. Proc.* **1997**, *468*, 305. (d) Leitner, J. *J. Phys. Chem. Solids* **1997**, *58*, 1329.

(8) Osamura, K.; Naka, S.; Murakami, Y. *J. Appl. Phys.* **1975**, *46*, 3432.

(9) (a) Nöth, H.; Konrad, P. *Z. Naturforsch.* **1975**, *30b*, 681. (b) Waggoner, K. M.; Olmstead, M. M.; Power, P. P. *Polyhedron* **1990**, *9*, 257.

(10) Crystallographic data for planar dimer $[M(NMe_2)_3]_2$, M = Al/Ga(1/1) (295 K): $C_{12}H_{36}N_6AlGa$, M_r = 361.17, triclinic, space group $P\bar{1}$(no. 2), a = 7.485(3) Å, b = 8.668(3) Å, c = 8.879(3) Å, α = 60.64(2)°, β = 84.55(3)°, γ = 88.11(3)°, V = 499.8(3) Å^3, $F(000)$ = 194, Z = 1, D_c = 1.200 g/cm^3, μ = 14.2 cm^{-1}, specimen size (mm) 0.30 × 0.40 × 0.50, 1512 reflections collected, 1389 unique reflections (R_{int} = 0.0201), 2θ range for data collection, 3.5−46.0°, scan type $\omega/2\theta$. All non-hydrogen atoms were refined anisotropically. Due to the high thermal motion of the methyl carbon atoms, hydrogen atoms were not included. The final cycle of full-matrix least-squares refinement was based on 1126 observed reflections ($I > 2\sigma(I)$) and 91 variable parameters and converged (largest parameter shift was 0.0022 times its esd) with final residual values of R = 0.0532, R_w = 0.0689, and S = 1.97. Refinement in the noncentrosymmetric space group, $P1$, resulted in a disordered model that was experimentally equivalent to the structure obtained in $P\bar{1}$. Selected distances (Å): M−(μ-N), 2.002 (av); M−(*exo*-N), 1.828(8); N−C, 1.48 (av). Ring angle: M−(μ-N)−M, 91.5°. A thermal ellipsoid diagram, the bond distances and angles, and the acquisition parameters are included in Supporting Information.

(11) (a) Sheldrick, G. M. *SHELXTL, Crystallographic Computing System*, Nicolet Instruments Division: Madison, WI, 1986. (b) *International Tables for X-ray Crystallography*, The Kynoch Press: Birmingham, England, 1974.

(12) Klug, P. H.; Alexander, E. L. In *X-ray Diffraction Procedures*; John Wiley & Sons: New York 1974; p 656 and references therein.

(vw), 2927 (w), 2958 (w), 3200−3250 (w). EA (%): C, 5.89; H, 5.43; N, 37.59; H*/N* (i.e., excluding H and N in NMe_2), 1.62. TGA (weight loss): 30−250 °C, 15%; 250−450 °C, 5%.

Equilibration in the System $[Al(NMe_2)_3]_2/[Ga(NMe_2)_3]_2$ and Formation of the Mixed-Metal Compound $(Me_2N)_2Al(\mu\text{-}NMe_2)_2Ga(NMe_2)_2$. Reference data (this study) for $[Al(NMe_2)_3]_2$: ^{1}H NMR (toluene-d_8/hexane-d_{14}): δ 2.34/2.50 (12H, μ-NMe_2), 2.68/2.54 (24H, *exo*-NMe_2); $^{13}C\{^1H\}$ NMR (toluene-d_8/hexane-d_{14}): δ 42.0/41.5 (*exo*-NMe_2), 42.2/42.4 (μ-NMe_2). Reference data (this study) for $[Ga(NMe_2)_3]_2$: ^{1}H NMR (toluene-d_8/hexane-d_{14}): δ 2.47/2.62 (12H, μ-NMe_2), 2.81/2.67 (24H, *exo*-NMe_2); $^{13}C\{^1H\}$ NMR (toluene-d_8/hexane-d_{14}): δ 44.0/43.5 (*exo*-NMe_2), 44.2/44.3 (μ-NMe_2). For a 1/1 solution of $[Al(NMe_2)_3]_2$ (0.0318 g or 0.1 mmol) and $[Ga(NMe_2)_3]_2$ (0.0404 g or 0.1 mmol) in 0.7 mL of a solvent, three additional ^{1}H NMR peaks of equal integrated areas were seen at δ (toluene-d_8/hexane-d_{14}) 2.40/2.55, 2.71/2.56, and 2.79/2.67 that were tentatively assigned, respectively, to the *exo*-$Al(NMe_2)_2$ (12H), $Al(\mu\text{-}NMe_2)_2Ga$ (12H), and *exo*-$Ga(NMe_2)_2$ (12H) in the mixed-metal $[(Me_2N)_2Al(\mu\text{-}NMe_2)_2Ga(NMe_2)_2]_2$. The $^{13}C\{^1H\}$ NMR peaks for this compound were at δ (toluene-d_8/hexane-d_{14}) 41.9/41.4, 43.2/43.3, and 43.9/43.6. For a fresh toluene-d_8 solution of the 1/1 bimetallic mixture, room-temperature ^{1}H NMR spectra were acquired at different times after preparation; the spectra were integrated and expressed in terms of the percentage of the equilibration product in the solution: 15 min, <1%; 2 h, 3%; 18 h, 28%; 48 h, 49%; and 112 h, 53%. The remaining resonances were those of the distinct $[Al(NMe_2)_3]_2$ and $[Ga(NMe_2)_3]_2$ in an approximate 1/1 ratio. Similar results were obtained for parallel studies in benzene-d_6 and hexane-d_{14}. Another fresh toluene-d_8 solution of the 1/1 mixture was used in a ^{1}H VT NMR experiment which yielded the following contents of the equilibration product (in parentheses, holding time at a given temperature): 25 °C (1.5 h), 3%; 55 °C (10 min), 10%; 55 °C (0.5 h), 22%; 55 °C (1 h), 35%, 55 °C (2 h), 52%; 90 °C (0.5 h), 53%; cooled to 25 °C (1 h), 53%; 25 °C (24 h), 53%; the resonances for the remaining $[Al(NMe_2)_3]_2$ and $[Ga(NMe_2)_3]_2$ integrated in a 1/1 ratio. Suitable X-ray quality crystals[10] were obtained at −30 °C from the fully equilibrated solution of $[Al(NMe_2)_3]_2$ and $[Ga(NMe_2)_3]_2$ in hexane (0.15 M each); MS for crystalline solid: *m/e* (intensity) (ion) clusters of peaks around 359 (24) ($AlGa(NMe_2)_6$ − H or M − H), 315 (47) (M − NMe_2), 273 (73) (M − $2NMe_2$ + H; possible contribution from $Al_2(NMe_2)_5$), 228 (100) (M − $3NMe_3$), 203 (8) ($Al(NMe_2)_4$; possible contribution from $Ga(NMe_2)_3$), 187 (6) ($Ga(NMe_2)_2(NMe)$; possible contribution from $Al(NMe_2)_3$-(NMe)), 158 (12) ($Ga(NMe_2)_2$ + H; possible contribution from $Al(NMe_2)_3$), 115 (4) ($Al(NMe_2)_2$), 44 (6) (NMe_2). Mp 89−91 °C.

Transamination in the Bimetallic System $[Al(NMe_2)_3]_2/[Ga(NMe_2)_3]_2$, Al/Ga = 1/1. Preparation of Precursor 1. Samples of $[Ga(NMe_2)_3]_2$, 2.02 g (5.0 mmol), and $[Al(NMe_2)_3]_2$, 1.59 g (5.0 mmol), were dissolved together in 30 mL of hexane and stirred at room temperature for 2 h. This was equivalent to the formation of about 3% of the mixed-metal compound (see above). Liquid (30 mL) NH_3 was transferred onto the solution at −78 °C forming an immiscible liquid phase with hexane. The mixture was stirred at −78 °C for 2 h, which was followed by a 2-h NH_3 boil-off at −33 °C. The hexane slurry was then stirred overnight at room temperature. The volatiles were removed, and the resulting white solid was evacuated for 2 h. EA (%): C, 10.82; H, 4.27; N, 24.78; H*/N* (i.e., excluding H and N in NMe_2), 1.16. IR (cm^{-1}), broad bands: 579 (s), 671 (s), 714 (s), 930 (m), 1513 (w, sh), 1544 (m), 2855 (vw), 2923 (w), 2960 (w, sh), 3200 (w).

Preparation of Precursor 2. Samples of $[Ga(NMe_2)_3]_2$, 2.02 g (5.0 mmol), and $[Al(NMe_2)_3]_2$, 1.59 g (5.0 mmol), were dissolved together in 30 mL of pentane and stirred at room temperature for 14 h. The volatiles were removed, and a benzene-d_6 sample of the solid was prepared. Based on ^{1}H NMR, it contained about 20% of the mixed-metal compound. Liquid (30 mL) NH_3 was deposited at −78 °C onto the isolated solid, and the mixture was stirred at this temperature for 2 h. The NH_3 was boiled off at −33 °C in 2 h, and the solid product was evacuated overnight. EA (%): C, 4.64; H, 3.95; N, 30.57; H*/N* (i.e., excluding H and N in NMe_2), 1.38. IR (cm^{-1}), broad bands: 575 (s), 690 (s), 720 (sh), 930 (s), 1250 (w), 1515 (sh), 1545 (m), 2857 (vw), 2955 (w), 3230 (w).

Preparation of Precursor 3. Samples of $[Ga(NMe_2)_3]_2$, 2.02 g (5.0 mmol), and $[Al(NMe_2)_3]_2$, 1.59 g (5.0 mmol), were dissolved together in 30 mL of pentane and refluxed for 3 h. The volatiles were removed, and a benzene-d_6 sample of the solid was prepared. Based on ^{1}H NMR, it contained about 40% of the mixed-metal compound. Liquid (30 mL) NH_3 was transferred at −78 °C onto the solid, and the mixture was refluxed in liquid NH_3 for 6 h. The volatiles were removed, and the solid was evacuated overnight. EA (%): C, 6.63; H, 3.68; N, 24.05; H*/N* (i.e., excluding H and N in NMe_2), 1.39. IR (cm^{-1}), broad bands: 575 (s), 675 (s), 929 (s), 1249 (w), 1380 (vw), 1515 (sh), 1545 (m), 2856 (vw), 2955 (w), 3200 (w). TGA (weight loss): 30−250 °C, 5.9%; 250−450 °C, 3.3%.

Preparation of Precursor 4. Samples of $[Ga(NMe_2)_3]_2$, 2.02 g (5.0 mmol), and $[Al(NMe_2)_3]_2$, 1.59 g (5.0 mmol), were dissolved together in 30 mL of hexane and refluxed for 3 h. This was equivalent to about 53% of the mixed-metal compound in the solution. Liquid (30 mL)NH_3 was transferred onto it at −78 °C, and the mixture was refluxed in liquid NH_3 for 6 h. The volatiles were removed, and the white product was evacuated for 2 h. EA (%): C, 2.73; H, 3.28; N, 29.33; H*/N* (i.e., excluding H and N in NMe_2), 1.29. IR (cm^{-1}), broad bands: 583 (s), 679 (s), 926 (s), 1246 (w), 1515 (sh), 1545 (m), 2928 (w), 2956 (w), 3190 (m). TGA (weight loss): 30−240 °C, 5.1%; 250−450 °C, 0.8%.

Pyrolysis Studies. Bimetallic Al/Ga−amide−imide precursors **1**−**4** as well as the Al−amide−imide and Ga−imide[4a] precursors were used in pyrolysis experiments. Preliminary pyrolyses under vacuum at 700 and 900 °C resulted in carbon-containing black products and were discontinued. All subsequent experiments were performed under a flow of NH_3 at 700, 900, and 1100 °C for precursors loaded in a quartz boat. At pyrolysis temperatures of 900 and, especially, 1100 °C, some corrosion of the boat's contact surface occurred (flaking), but the bulk product was apparently unaffected by interaction with silica. The most commonly used heating scheme consisted of preheating at 150 °C (1 h), ramping (15 min) to the final temperature at 700, 900, or 1100 °C, and holding for 3 h. Some samples, indicated with a pound sign (#) in sections **a**−**c** below, were also pyrolyzed using the following heating steps (in parentheses, holding time at the given temperature): 150 °C (0.5 h), 400 °C (0.5 h), 600 °C (2 h), and final temperature at 700 or 900 °C. The products were light-colored, yellow to light gray solids. They all were characterized by XRD spectroscopy, many by EA, IR, and PL methods, and selected ones by TEM/EDS techniques.

(a) Pyrolysis of Ga−Imide To Afford GaN: 700 °C, yellow. XRD, cubic/hexagonal GaN (D = 5 nm). 700 °C,# yellow. XRD, cubic/hexagonal GaN (D = 6 nm). 900 °C,# yellow. XRD, hexagonal GaN (D = 21 nm). 1100 °C, yellow. IR (cm^{-1}): 580 (br). XRD, hexagonal GaN (D = 23 nm).

(b) Pyrolysis of Al−Amide−Imide To Afford AlN: 900 °C, light gray. XRD, hexagonal AlN (D = 5 nm). 1100 °C, light gray. EA (%) found (calcd for AlN): N, 33.78 (34.17); C, < 0.3 (0); H, < 0.1 (0). IR (cm^{-1}): 680 (br). XRD, hexagonal AlN (D = 10 nm).

(c) Pyrolysis of Al/Ga−Amide−Imide Precursors 1−4 To Afford Composites. In the XRD diffractograms of some of the materials pyrolyzed at 1100 °C, two partially overlapped hexagonal patterns are discernible: one with sharp, high-intensity peaks (GaN-type) and the other with very broad, much less intense peaks (AlN-type). In one favorable case, two calculated average particle sizes, D(sharp)/D(broad), D_s/D_b, are included (vide infra). Precursor **1**: 700 °C, gray; IR (cm^{-1}): 700 (br). XRD, cubic/hexagonal (D = 4 nm). 700 °C,# gray. EA (%) found (calcd for $AlGaN_2$): N, 22.18 (22.46); C, 0.73 (0); H, 0.34 (0). XRD, cubic/hexagonal (D = 5 nm). 900 °C, light gray. EA (%) found (calcd for $AlGaN_2$): N, 20.29 (22.46); C, 0.21 (0); H, 0.16 (0). XRD, hexagonal (D = 13 nm).

900 °C,[#] light gray. EA (%) found (calcd for $AlGaN_2$): Ga, 52.57 (55.90); Al, 21.98 (21.63); N, 20.42 (22.46); C, 0.25 (0); H, 0.20 (0); Al/Ga = 1.08. XRD, hexagonal (D = 15 nm). 1100 °C, light gray. IR (cm^{-1}): 675 (br), 600 (sh). XRD, hexagonal (D = 18 nm). Precursor **2**: 900 °C, light gray. IR (cm^{-1}): 675 (br), 600 (sh). XRD, hexagonal (D = 20 nm). 1100 °C, light gray. XRD, hexagonal (D = 23 nm). Precursor **3**: 900 °C, light gray. IR (cm^{-1}): 670 (br), 590 (sh). XRD, hexagonal (D = 18 nm). 1100 °C, light gray. EA (%) found (calcd for $AlGaN_2$): N, 21.95 (22.46); C, < 0.1 (0); H, < 0.1 (0). IR (cm^{-1}): 670 (br), 615 (sh). XRD, hexagonal (D = 20 nm). Precursor **4**: 700 °C, light gray. EA (%) found (calcd for $AlGaN_2$): N, 22.19 (22.46); C, 0.33 (0); H, 0.24 (0). IR (cm^{-1}), broad bands: 3225 (w), 2168 (w), 920 (w), 679 (s), 594 (s). XRD, cubic/hexagonal (D = 6 nm). 900 °C, light gray. IR (cm^{-1}), broad bands: 675 (s); 595 (s). XRD, hexagonal (D = 13 nm). 1100 °C, light gray. EA (%) found (calcd for $AlGaN_2$): N, 20.17 (22.46); C, 0.20 (0); H, 0.10 (0). IR (cm^{-1}): 675 (br), 600 (sh). XRD, hexagonal (D_s/D_b = 15 nm/8 nm).

Results and Discussion

Nanocrystalline AlN via Transamination/Deamination of $[Al(NMe_2)_3]_2$. The reactions between $[Al(NMe_2)_3]_2$ and liquid NH_3 resulted in an advantageous precursor whose chemical makeup was consistent with the polymeric Al−amide−imide $[Al(NH_2)(NH)]_n$, containing some residual NMe_2 groups (eq 1). The EA data yielded an H/N ratio of 1.62 (excluding NMe_2 groups estimated from the C content) vs 1.50 for the Al−amide−imide. IR spectroscopy also provided strong structural evidence by displaying, in addition to weak NMe_2-associated bands, a signature band at 1545 cm^{-1} (NH_2) with the distinct shoulder at 1515 cm^{-1} (NH) for the NH_2/NH groupings in $[Al(NH_2)(NH)]_n$.[6b] The number of residual NMe_2 groups could be estimated from the EA data and amounted to about one such group per eight aluminum atoms. The total TGA weight loss of 20% for the material was lower than the calculated 29.4% for the Al−amide−imide; continued deamination in the fresh precursor could be partly responsible for the discrepancy.

The pyrolysis of the Al−amide−imide was initially carried out under vacuum and resulted in a black solid that was shown by XRD spectroscopy to be hexagonal AlN. The black tinge indicated a high level of carbon retained in the product. The pyrolysis of the Al−amide−imide to light gray, nanocrystalline AlN was successfully performed at 900 and 1100 °C under NH_3 flow, a treatment which is known to substantially remove NR_2 carbons as HNR_2 and improve the product's crystallinity.[13] A partial elemental analysis was done for the latter material and showed a satisfactory N content and C and H contents below detection limits of the applied analytical procedures, consistent with high-purity AlN. The IR broad band at 680 cm^{-1} was typical for AlN. The products were shown by XRD to be hexagonal, 2H-wurtzite AlN (JCPDS file 25-1133; reported: a = 3.111 Å, c = 4.979 Å). Due to the broadness of the pattern, accurate calculations of a and c were not attempted. Approximate determinations were done, however, using Bragg's equation, the (002) diffraction for c, and the (110) diffraction for a; the estimated values were a = 3.11 Å and c = 4.96 Å and agreed satisfactorily with those reported for AlN. The crystallite sizes averaged 5 nm (900 °C) and 10 nm (1100 °C).

Equilibration in the System $[Al(NMe_2)_3]_2$/$[Ga(NMe_2)_3]_2$, Al/Ga = 1/1. The encouraging results for the separate transaminations of $[Al(NMe_2)_3]_2$ and $[Ga(NMe_2)_3]_2$[4a] prompted us to look into the mixed system composed of these two compounds. We first studied possible exchange processes taking place in toluene, benzene, or hexane solutions containing equimolar quantities of the compounds as the means to preforming the Al−N(Me_2)−Ga bridges. Indeed, we discovered that the solutions were involved in exchanges leading to the formation of the homoleptic four-membered-ring compound $(Me_2N)_2Al(\mu\text{-}NMe_2)_2Ga(NMe_2)_2$ in admixture with separate $[Al(NMe_2)_3]_2$ and $[Ga(NMe_2)_3]_2$, stable on the NMR time scale (vide infra, Scheme 1). For example, a typical ^1H NMR spectrum in toluene-d_8 showed, in addition to the resonances for the distinct parent dimers, three new peaks at δ 2.40, 2.71, and 2.79 that grew with time, which were tentatively assigned, on the basis of a comparison with the signals for the parent dimers, respectively, to the *exo*-$Al(NMe_2)_2$, $Al(\mu\text{-}NMe_2)_2$-Ga, and *exo*-$Ga(NMe_2)_2$ protons in the equilibration product $(Me_2N)_2Al(\mu\text{-}NMe_2)_2Ga(NMe_2)_2$. Some support for the existence of the mixed-metal compound also in the solid state came from the mass spectrum obtained for the crystalline equilibration product. The highest m/e cluster of peaks in the spectrum was found at m/e 359, i.e., 1 unit smaller than the parent ion for the mixed-metal compound at m/e 360.

The solution system appeared to reach equilibrium at about 53% content of the mixed-metal compound and equimolar quantities of the separate initial dimers after a few days at room temperature. On the other hand, a similar equilibrium level was reached after only 2 h if the fresh toluene solution was heated to 55 °C. Once reached, this level seemed to remain stable within the accuracy of our determinations in the temperature range from 25 to 90 °C or in the course of several days at room temperature. The solid that crystallized from the equilibrated solution, which was subsequently redissolved in benzene-d_6, was shown by NMR spectroscopy to consist of the same equilibrated species as seen before crystallization, i.e., about 53% of mixed-metal $(Me_2N)_2Al(\mu\text{-}NMe_2)_2Ga(NMe_2)_2$ and equimolar $[Al(NMe_2)_3]_2$ and $[Ga(NMe_2)_3]_2$.

An X-ray single-crystal structure determination was attempted for the solid that crystallized in this bimetallic system to further address the question of equilibration products. The obtained structure features a planar four-membered ring with the {M−N−M−N} core.[10] This compares well with the structures known for the parent dimers $[Al(NMe_2)_3]_2$[9b,14] and $[Ga(NMe_2)_3]_2$.[9b] The centrosymmetric space group of the crystallographic solution requires that the unique metal site M represent a 50% occupation by both Al and Ga atoms. In general, such a structural solution could originate either from the {Al−N−Ga−N} alternating cores in packing stacks or from intimately cocrystallized separate dimers [Al-

(13) For example, see the following: (a) Sauls, F. C.; Hurley, W. J.; Interrante, L. V.; Marchetti, P. S.; Maciel, G. E. *Chem. Mater.* **1995**, *7*, 1361. (b) Paine R. T. In *Inorganometallic Chemistry*; Fehlner, T. P., Ed.; Plenum Press: New York, 1992; p 359 and references therein. (c) Koyama, S.; Takeda, H.; Saito, Y.; Sugahara, Y.; Kuroda, K. *J. Mater. Chem.* **1996**, *6*, 1055.

(14) Ouzounis, K.; Riffel, H.; Hess, H.; Kohler, U.; Weidlein, J. *Z. Anorg. Allg. Chem.* **1983**, *504*, 67.

Scheme 1

1. Equilibration in hexane solution:

$$\underset{\text{I}}{[Al(NMe_2)_3]_2} + \underset{\text{II}}{[Ga(NMe_2)_3]_2} \rightleftharpoons \underset{\text{III}}{(Me_2N)_2Al(\mu\text{-}NMe_2)_2Ga(NMe_2)_2}$$

2. Reactions of equimolar I and II and varying amounts of III with NH_3: (I + II + III = 100%)

I + II + III (3%); hexane solution	NH_3	precursor **1**
I + II + III (20%); solid state		precursor **2**
I + II + III (40%); solid state		precursor **3**
I + II + III (53%); hexane solution		precursor **4**

$(NMe_2)_3]_2$ and $[Ga(NMe_2)_3]_2$, or from both the cocrystallized separate dimers and the mixed-metal compound. Regardless of the intrinsic limitations in their interpretation, the structural data are consistent with an efficient mixing of the species on the molecular level.

Aluminum/Gallium Nitride Nanocomposites via Transamination/Deamination in the System $[M(NMe_2)_3]_2/NH_3$, M = Al/Ga (1/1). Transamination/deamination in the system $[M(NMe_2)_3]_2/NH_3$, M = Al/Ga (1/1), was performed for the reactants preequilibrated in hexane or pentane at various levels, i.e., 3%, 20%, 40%, and 53% of the mixed-metal compound. They were either isolated as solids by evacuation of the solvent (20% and 40% cases) or remained in the solution (3% and 53% cases) for reaction with liquid NH_3. Following the condensation of NH_3 at −78 °C, the system was warmed to about −33 °C, at which point NH_3 was refluxed and/or allowed to slowly boil off. This was followed by evacuation at room temperature and resulted in precursors **1**−4 as summarized in Scheme 1. All four precursors contained abundant NH_2/NH groups and small quantities of residual NMe_2 groups, as inferred from the EA and IR data. For reference purposes below, a 1:1 mixture of $[Al(NH_2)(NH)]_n$ (H/N, 1.50) and $[Ga(NH)_{3/2}]_n$ (H/N, 1.00) would show H/N at about 1.29. Precursor **1** (3% case) had a C content of 10.82% and a H*/N* (i.e., excluding H and N in NMe_2) ratio of 1.16. This could be compared with precursor **4** (53% case) showing a C content of 2.73% and a H*/N* ratio equal to 1.29, a striking match with the reference value above. The precursors obtained from the reactions between NH_3 and isolated solids **2** (20% case) and **3** (40% case) showed these values: (**2**) C, 4.64; H*/N*, 1.38. (**3**) C, 6.63; H*/N*, 1.39. It would seem that precursor **4** was the most deeply converted toward Al/Ga−imide−imide. All these precursors might be envisioned as having some proportion of mixed cross-linking resulting, for instance, from transamination [Al−N(Me$_2$)−Ga + NH_3 = Al−N(H$_2$)−Ga + $HNMe_2$] or deamination [Al−NMe_2 + H_2N−Ga = Al−N(H)-Ga + $HNMe_2$]. The extent of it, in the first approximation, could perhaps be related to the progress of equilibration in the bimetallic system $[Al(NMe_2)_3]_2/[Ga(NMe_2)_3]_2$ via formation of the mixed Al−N(Me$_2$)−Ga linkages.

The precursors were pyrolyzed under a NH_3 flow, independently at 700 (some precursors), 900, and 1100 °C resulting in light gray composites. These temperature limits were set as a compromise between efficient conversion/crystallization rates and thermal stabilities of the nitrides. Despite some inconsistencies in the literature,[15] AlN appears be stable even at 1700 °C, while GaN apparently decomposes above 1000−1100 °C. Temperatures higher than 700 °C should have promoted

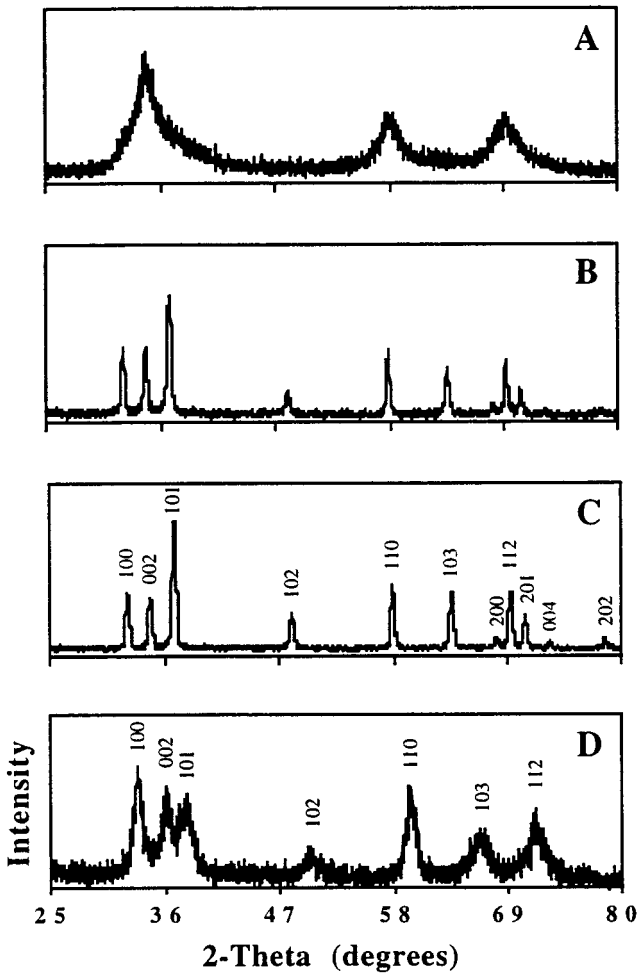

Figure 1. XRD patterns for pure nitrides GaN and AlN obtained, respectively, from gallium imide and aluminum amide imide at different temperatures: **(A)** GaN, 700 °C; **(B)** GaN, 900 °C; **(C)** GaN, 1100 °C; **(D)** AlN, 1100 °C.

the formation of hexagonal GaN as opposed to the preferred cubic/hexagonal variety observed at lower temperatures,[4,16] and this could be beneficial for alloying with hexagonal AlN. The products showed very low residual C and H contents and N contents in the 20.17−22.19% range, close to the expected value for the $AlGaN_2$ composition, 22.46%. The IR spectra for the products (900 and 1100 °C) were quite similar, displaying one broad band centered at 670−680 cm^{-1} (Al−N stretch) with a distinct shoulder at 580−600 cm^{-1} (Ga−N stretch).

The reference XRD patterns obtained in this study for pure nitrides (Figure 1) and for an approximately 1:1 physical mixture of AlN and GaN (Figure 2C) illustrate the general appearance of the diffractograms; note the much less intense patterns for AlN, a result of the pronounced peak broadness associated with the material's extreme nanocrystallinity. The XRD patterns were also obtained for all composites, and generally, they displayed two distinct characteristics depending on pyrolysis temperature. For materials heated at 700 °C,

(15) (a) Lyutaya, M. D.; Bartnitskaya, T. S. *Inorg. Mater. (Transl. of Neorg. Mater.)* **1973**, *9* (7), 1052 (Russian version, p 1186). (b) Neumayer, D. A.; Ekerdt, J. G. *Chem. Mater.* **1996**, *8*, 9 and references therein.

(16) Hwang, J.-W.; Campbell, J. P.; Kozubowski, J.; Hanson, S. A.; Evans, J. F.; Gladfelter, W. L. *Chem. Mater.* **1995**, *7*, 517.

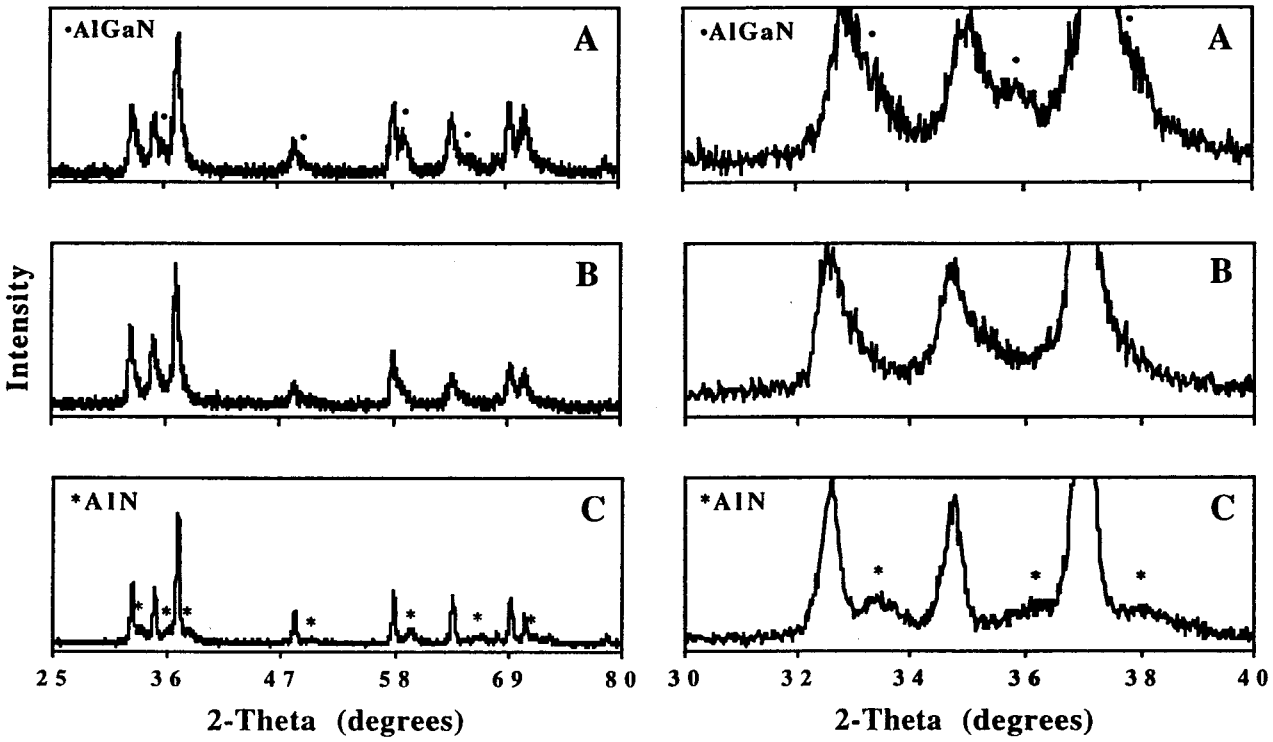

Figure 2. XRD patterns for precursors pyrolyzed at 1100 °C; right side, expansion of the 2θ 30−40° region: **(A)** composite from precursor **4** (AlGaN stands for aluminum/gallium nitride solid solution phase); **(B)** composite from precursor **1**; **(C)** AlN/GaN, 1/1 physical mixture.

the patterns were consistent with a nanocrystalline, cubic/hexagonal phase of GaN as previously observed for pyrolysis of the Ga−imide[4] or by comparison with pure GaN from pyrolysis at 700 °C in this study (Figure 1A). On the other hand, samples pyrolyzed at 900 and 1100 °C showed a rather sharp, strong hexagonal pattern of the GaN type (improved for 1100 °C) but also a second, much broader and less intense frequently superimposed hexagonal pattern that appeared to be derived from the AlN lattice.

This is illustrated in Figure 2 where three XRD patterns, all related to the pyrolysis of different precursors at 1100 °C, are included. Figure 2 on the right shows the expansions of the 2θ 30−40° region. It is clear that the GaN type pattern (sharp lines) is severely superimposed over the AlN type pattern (broad lines). For example, in spectrum B for precursor **1**, a severe overlap of the two types of patterns takes place and results in broadening of the sharp peaks' bases beyond distinct separation. The AlN type component in spectrum A is not pure AlN because it shows different peak positions than those for the AlN reference. Figure 3 shows the XRD patterns for the composites obtained from precursor **4** at 700, 900, and 1100 °C and illustrates the temperature-related effect on the patterns.

Table 1 summarizes the average crystallite sizes and rough estimates of lattice parameters, whenever possible, and the latter were done using Bragg's equation, the (002) diffraction for *c*, and the (110) diffraction for *a*, as discussed earlier for pure AlN. For example, for precursor **4**, the biggest change in the average crystallite size for the GaN type component is noticed when going from 700 °C (not shown in Table 1), 6 nm, to 900 °C, 13 nm; a much smaller change is seen when going to 1100 °C, 15 nm. The comparison of the lattice parameters

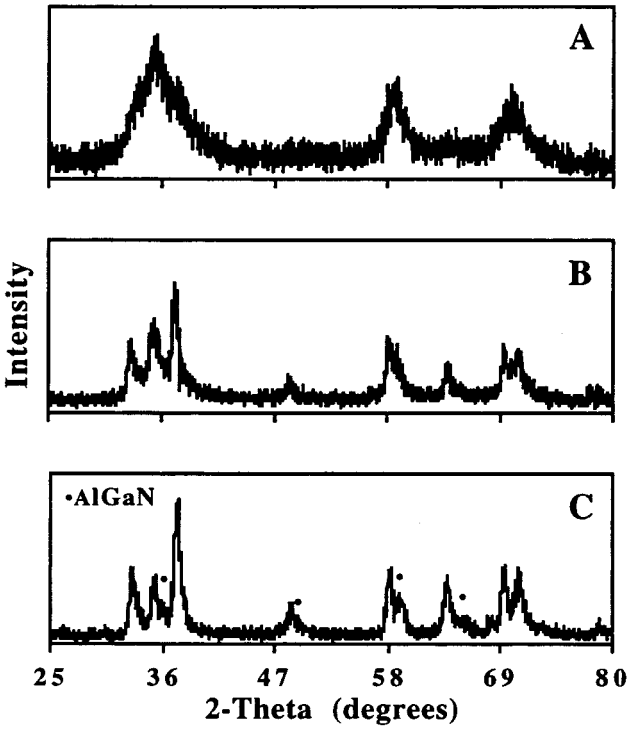

Figure 3. XRD patterns for composites obtained from precursor **4** at different pyrolysis temperatures: **(A)** 700 °C; **(B)** 900 °C; **(C)** 1100 °C (AlGaN stands for aluminum/gallium nitride solid solution phase).

for the GaN type with those for pure GaN shows that they approach each other, especially for composites pyrolized at 1100 °C. Regarding the second identified component, the AlN type lattice, both *a* and *c* are close to the average values for pure AlN and pure GaN, which, according to Vegard's law, indicates an AlGaN

Table 1. Average Particle Sizes (*D*) and Estimated Lattice Parameters (*a*, *c*) Derived from XRD Patterns for Hexagonal Phases in Composites and Pure Nitrides

	900 °C						1100 °C					
	composite from precursor						composite from precursor					
	1	**2**	**3**	**4**	GaN	AlN	**1**	**2**	**3**	**4**	GaN	AlN
average size, *D* (nm)	13	20	18	13	21	5	18	23	20	15/8	23	10
GaN-type, *a* (Å)	3.16	3.18	3.18	3.17	3.19		3.18	3.18	3.18	3.17	3.18	
c (Å)	5.13	5.16	5.14	5.12	5.19		5.16	5.15	5.15	5.16	5.17	
AlN-type, *a* (Å)		3.15	3.14	3.14		3.09	3.15	3.14	3.13	3.13		3.11
c (Å)				5.05		4.93	5.09	5.05	5.06	5.06		4.96

solid solution with equal proportions of Al and Ga. This can be compared with the report (not detailed, though) on bulk solid solutions of AlN and GaN[15a] in which the 1:1 solution is quoted to have the GaN type of hexagonal lattice. It is also interesting to note that, strictly on the basis of mass balance considerations, the presence of pure GaN (GaN type) with the concurrent 1:1 Al/Ga solid solution (AlN type) requires a third, aluminum-rich phase, possibly pure AlN. This nanophase in small quantities would not be easily seen by XRD due to its extreme peak broadness and overlap with the major spectral components. In summary, the XRD data suggest that there are two or three distinct hexagonal phases in these composites that differ quite significantly in their average particle sizes and compositions.

TEM/EDS measurements were undertaken to probe the composites from another angle. Figures 4 and 5 show typical grain habit/crystallinity and electron diffraction patterns. In general, the samples pyrolyzed at 700 °C (for example, Figure 4A) are composed of quite uniformly sized particles with diameters less than several nanometers. They are crystalline, and the electron diffraction patterns show rather diffuse lines with infrequent spots consistent with basic nanocrystalline character. The EDS data for the material shown in Figure 4A provide relative Ga contents of 52−55% and Al contents of 45−48%. These estimates are consistent with equimolar Al/Ga ratios homogeneously distributed in the material. On the other hand, the samples prepared at 900 and 1100 °C are similar to each other and display an apparent bimodal size distribution. They show a fraction of very large crystallites, bigger than 80−100 nm, which are usually embedded in a matrix of particles smaller than 20−30 nm (for example, Figure 4B, left, and Figure 5, top). The electron diffraction patterns for the biggest particles from the pyrolysis at 1100 °C confirm their single-crystal nature (Figure 5, bottom, right), and EDS gives relative Ga contents higher than 95%, which may simply correspond to pure GaN. The electron diffraction pattern for the matrix particles in this material (Figure 5, bottom, left) shows the spotty rings reflecting polycrystallinity and particles bigger than several nanometers. The EDS data for the matrix in this sample provide relative Ga contents of 28−31% and Al contents of 69−72%, i.e., material on average enriched in aluminum. EDS results very similar to those discussed above were also obtained for both the large crystallites and the finer particles in the composite from precursor **1** pyrolyzed at 900 °C. These averaged EDS results for the matrix can be interpreted as describing a mixture of two separate homogeneously dispersed phases suggested earlier from the XRD data and mass balance considerations, i.e., one phase of the AlGaN solid solution with an Al/Ga ratio close to 1/1 and a postulated second phase of possibly pure AlN.

Some preliminary room-temperature photoluminescence (PL) measurements of the composites have been carried out employing an excitation wavelength of 325 nm, a value commonly used to excite the luminescence of homogeneous GaN materials (a bulk band gap of around 3.4 eV). The Xe lamp employed in our PL spectrometer does not possess sufficient power in the far-UV region necessary to excite the bulk band gap of AlN (6.2 eV) or any corresponding possible Al-rich nitride phases. As a consequence, the focus of these measurements is limited to an examination of gallium-rich nitride phases or pure GaN domains, if any. For a given pyrolysis temperature (for example, 900 °C), the composites from precursors **1**−**3** show similar PL spectra which are in stark contrast with the emission observed for the composites from precursor **4**. In the case of the nitride derived from pyrolysis of precursor **1** at 900 °C (Figure 6A), very broad emission centered around 550 nm is observed. While yellow-green defect PL in this type of sample apparently dominates the photophysics, one cannot rule out some contribution of weak band edge blue PL based on the substantial line width (fwhm, about 250 nm) of this emission. This conclusion is supported by the fact that pyrolysis of this same precursor at 1100 °C results in the shift in the defect feature to longer wavelength, making the detection of a distinct shoulder in the blue region more facile. Both of these PL features have been previously observed and their origin discussed for bulk nanophase GaN[4b,c] as well as in epitaxial thin films.[17] In contrast, spectra obtained for the composite from precursor **4** pyrolyzed at 900 °C (Figure 6B) show very strong blue emission at approximately 420 nm and a negligible yellow component. For these samples, there is a positive correlation between the relative intensity of the yellow emission and the pyrolysis temperature employed to convert the precursor to the nitride composite, with the most intense defect emission observed in samples pyrolyzed at 1100 °C. These data may be indicative of thermally generated lattice defects at temperatures approaching the reported thermal stability limits for GaN (1000−1100 °C). There are some differences in the relative intensities of the emission maxima among the composites, but no clear correlation is apparent from the data presented. In summary, the PL measurements are consistent with the presence of the GaN component

(17) (a) Ogino, T.; Aoki, M. *Jpn. J. Appl. Phys.* **1980**, *19*, 2395. (b) Hofman, D. M.; Kovalev, D.; Steude, G.; Meyer, B. K.; Hoffman, A.; Eckey, L.; Detchprom, T.; Amano, H.; Akasaki, I. *Phys. Rev. B* **1995**, *52*, 16702. (c) Glaser, E.; Kennedy, T.; Doverspike, K.; Rowland, L.; Gaskill, D.; Freitas, J.; Asif Khan, M.; Olson, D.; Kuznia, J.; Wickenden, D. *Phys. Rev. B* **1995**, *51*, 13326.

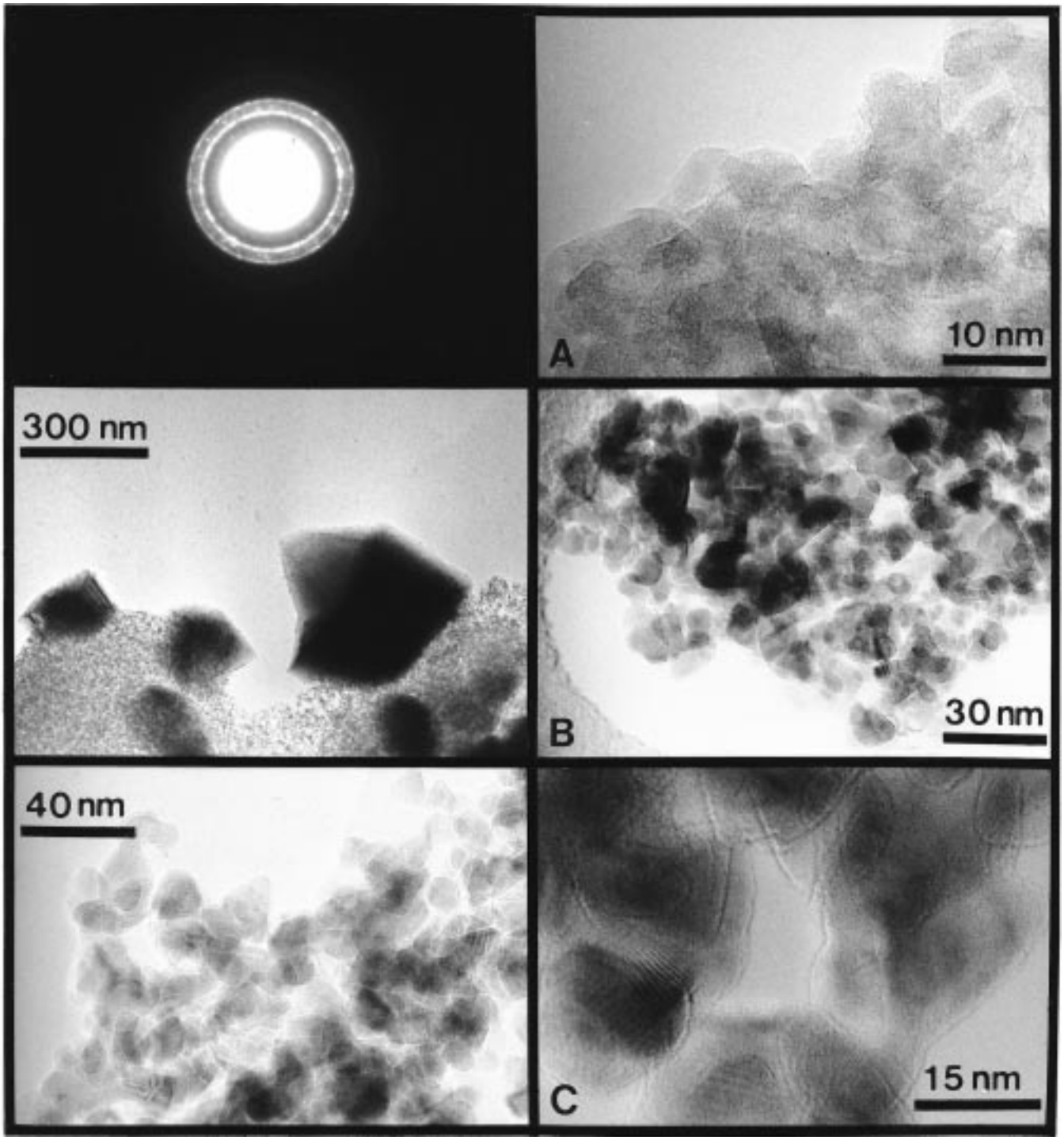

Figure 4. TEM images and electron diffraction pattern for composites obtained from precursor **4** at pyrolysis temperatures: **(A)** (top row) 700 °C, electron diffraction pattern (left) and HRTEM showing lattice fringes (right). **(B)** (middle row) 900 °C, low magnification (left) and high magnification of the small particle region (right). **(C)** (bottom row) 1100 °C, high magnification (left) and HRTEM showing lattice fringes (right) of the small particle region.

in these composites which we believe corresponds to the GaN type phase earlier emerging from the XRD and TEM/EDS data. We plan extended photoluminescence studies employing shorter excitation wavelengths which, coupled with Raman spectroscopy, will elucidate the character of other components of the composites.

The materials characterization results can be reconciled with the following nature of the synthesized nitride composites. First, the composites obtained at 700 °C seem to be prevailingly cubic/hexagonal nanolattices of the known phase-inhomogeneous GaN; no other distinct phases were detected on the several nanometer scale. These materials also appear to be chemically homogeneous on this scale. However, it is possible that there is some chemical and phase inhomogeneity on the smaller than a few nanometer scale which we were unable to probe. It is thus probable that the postulated second AlN-type component, possibly pure AlN, which may be emerging from the precursors' pyrolysis at this temperature is still not completely converted and of extremely small particle size. This is a viable supposition since, for the Al−amide−imide precursor pyrolyzed

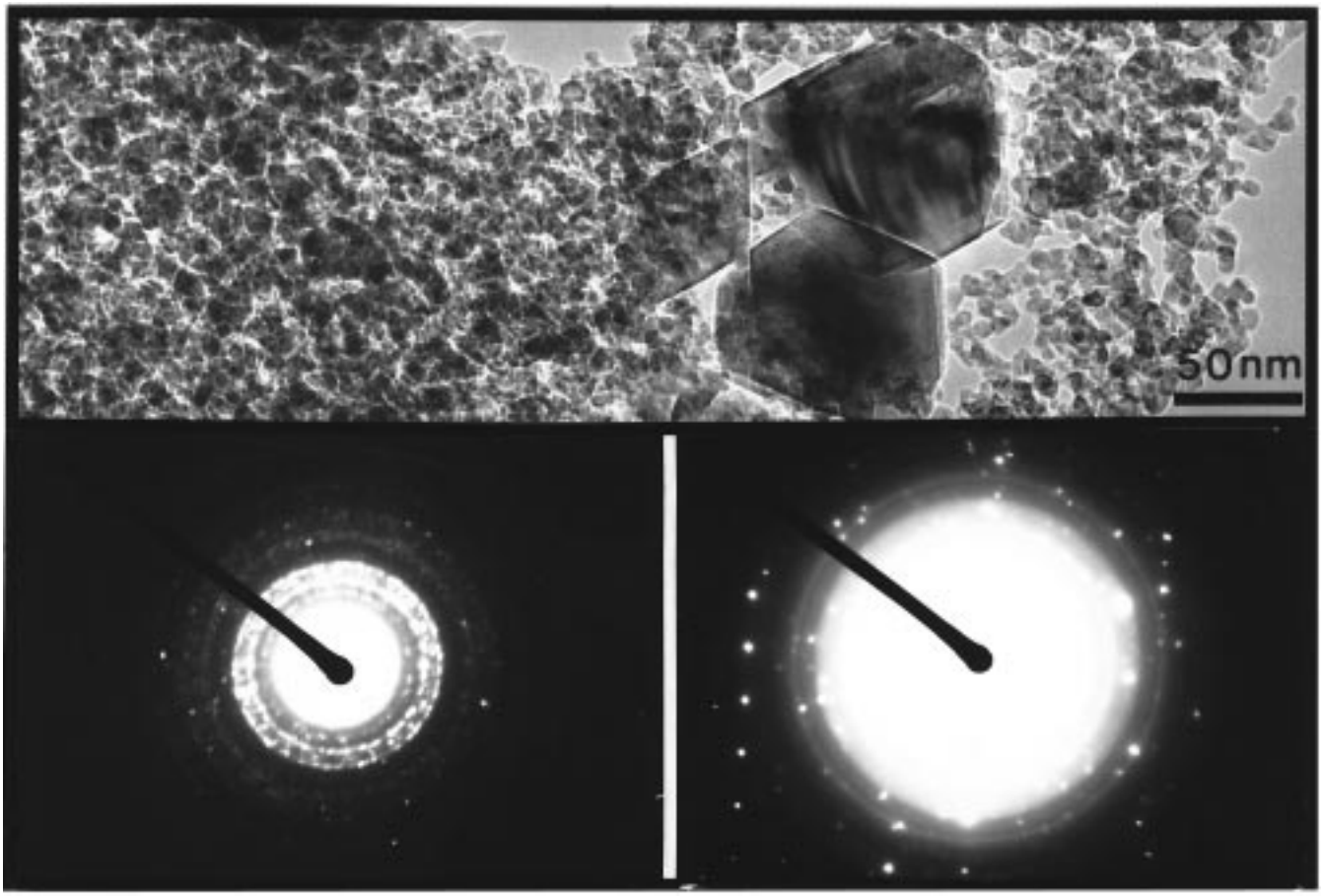

Figure 5. TEM image (top) and electron diffraction patterns (bottom left, small particles; bottom right, large crystallite) for composite from pyrolysis of precursor **3** at 1100 °C.

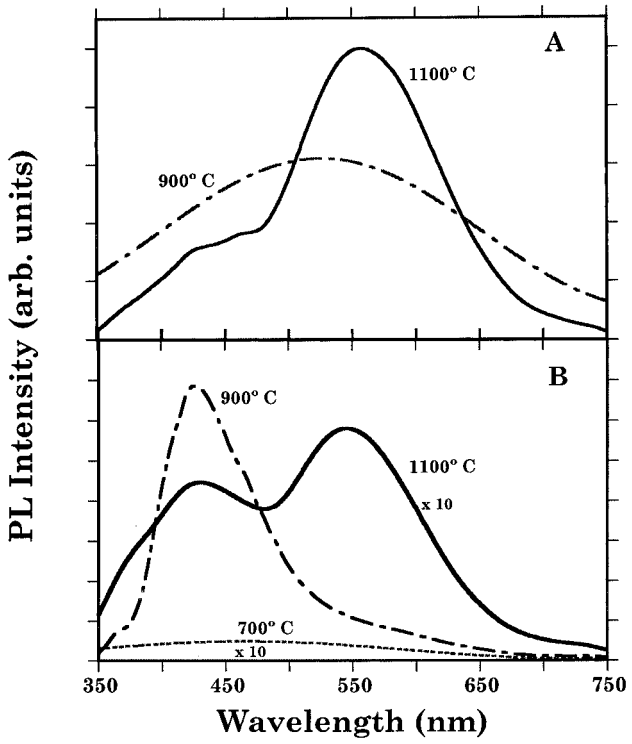

Figure 6. Room-temperature photoluminescence spectra at 325 nm excitation wavelength for composites obtained from precursors **1** (A) and **4** (B).

at 900 °C, the average particle size is only 5 nm and much smaller sizes would be expected at 700 °C. Such a structural makeup of the 700 °C composites could have escaped differentiation by XRD, EDS, and even standard HRTEM techniques. On the other hand, the composites obtained at 900 and 1100 °C have much in common, and the latter temperature is in their upper stability limits. These materials appear to be composed of at least two detected crystallographic hexagonal phases, pure GaN and AlGaN solid solution with Al/Ga approximately 1/1, and postulated pure AlN. The particles made of these phases form an apparent multimodal size distribution system. The smallest particles contain a mixture of pure AlN and AlGaN solid solution, while the largest particles appear to be pure GaN; some particles of the latter phase are very large, reaching more than 100 nm.

The picture emerging from the results and discussion above is consistent with the existence of a correlation between the chemical nature of the starting bimetallic Al/Ga−amide−imide precursors and the resulting makeup of the composites derived from them. The presence in an initial reaction mixture of three different species with distinct bonding situations, Ga−N(Me_2)−Ga, Al−N(Me_2)−Al, and mixed-metal Ga−N(Me_2)−Al, seems to lead upon transamination/deamination with NH_3 to a precursor preserving these three bonding domains, via transaminated nitrogen bridges. The following pyrolysis leads to elimination−condensation, to a large degree, separately within these three domains and formation at appropriate temperatures of three distinct hexagonal phases evolved from them. These

phases are consistent with AlN, GaN, and AlGaN (Al/Ga = 1/1) solid solution of aluminum/gallium nitride and directly reflect the chemical makeup of the precursor. Unfortunately, we were unable to confirm any clear quantitative trend among the different precursors in relation to the nature of the resulting composites. This is mainly due to inherent problems to quantify the results of the characterization methods which we used. We notice, however, that the most intense peaks of the AlN type (AlGaN solid solution) in the XRD spectra are obtained for the composites derived from precursors **3** and **4** but not **1**, i.e., for those containing significant mixed Al−N−Ga bridges, in qualitative agreement with the above. Further efforts are underway to address the quantitative aspect of composite formation as well as to perform extended characterization of the composites by photoluminescence at lower excitation wavelengths and by Raman spectroscopy.

Note Added in Proof. Since submission of this paper, a report on the proposed cubic AlGaN solid solution/polymer composite formation at 600 °C from a similar reaction system has been published.[18] Our paper appears to be complementary in that it addresses the chemical aspects of precursor formation and nature as well as deals with conversion temperatures higher than 600 °C. At the same time, it is somewhat controversial since we are reporting rather complex hexagonal aluminum/gallium nitride composites obtained under these conditions.

Acknowledgment. R.L.W. wishes to thank the Office of Naval Research for its financial support. J.L.C. thanks the Robert A. Welch Foundation for support. We also want to thank Dr. Serge Oktriabrsky from the North Carolina State University for his help in evaluating the TEM/EDS results.

Supporting Information Available: Thermal ellipsoid diagram; tables of bond distance and angles, anisotropic displacement coefficients, atomic fractional coordinates and *U* values, and observed and calculated structure factors for $[M(NMe_2)_3]_2$, M = Al/Ga(1/1) (9 pages). Ordering information is given on any current masthead page.

CM9708067

(18) Benaissa, M.; Gonsalves, K. E.; Rangarajan, S. P. *Appl. Phys. Lett.* **1997**, *71*, 3685.